Scientific Reports

https://doi.org/10.1038/s41598-026-35430-8

Article in Press

Development of a global screening system for detecting protein–protein interactions by luminescence complementation in fission yeast

Received: 17 September 2025

Accepted: 6 January 2026

Published online: 12 January 2026

Cite this article as: Azadeh F., Hashimoto A., Nishimura S. *et al.* Development of a global screening system for detecting protein–protein interactions by luminescence complementation in fission yeast. *Sci Rep* (2026). https://doi.org/10.1038/s41598-026-35430-8

Fereshteh Azadeh, Atsushi Hashimoto, Shinichi Nishimura, Manabu Arioka, Minoru Yoshida & Akihisa Matsuyama

Development of a global screening system for detecting protein-protein interactions by luminescence complementation in fission yeast

Fereshteh Azadeh[1,2§], Atsushi Hashimoto[2,3], Shinichi Nishimura[4], Manabu Arioka[1,5], Minoru Yoshida[1,2,5,6,7*], and Akihisa Matsuyama[1,2,3*]

[1]Laboratory of Microbiology, Department of Biotechnology, Graduate School of Agricultural and Life Sciences, The University of Tokyo, 1-1-1, Yayoi, Bunkyo-ku, Tokyo 113-8657, Japan

[2]Chemical Genomics Research Group, [3]Molecular Ligand Target Research Team, RIKEN Center for Sustainable Resource Science, 2-1, Hirosawa, Wako, Saitama 351-0198, Japan

[4]Graduate School of Integrated Sciences for Life, Hiroshima University, Higashi-Hiroshima, 739-8528, Japan

[5]Collaborative Research Institute for Innovative Microbiology (CRIIM), [6]Office of University Professors, The University of Tokyo, 1-1-1, Yayoi, Bunkyo-ku, Tokyo 113-8657, Japan

[7]Drug Discovery Seeds Development Unit, RIKEN Center for Sustainable Resource Science, 2-1, Hirosawa, Wako, Saitama 351-0198, Japan

*Co-corresponding authors

*Address for Co-corresponding authors: Molecular Ligand Target Research Team/Drug Discovery Seeds Development Unit, RIKEN Center for Sustainable Resource Science, 2-1, Hirosawa, Wako, Saitama 351-0198, Japan. Tel: +81-48-462-1111, e-mail: yoshidam@riken.jp, akihisa@riken.jp

§Present address: Systems Biology and Genome Engineering Section, National Human Genome Research Institute, BG 49 RM 4A82, 49 Convent DR, Bethesda MD 20892, Tel; +1 301-827-7012, email: fereshteh.azadeh@nih.gov

Keywords: *Schizosaccharomyces pombe*, interactome, protein complementation assay, NanoBiT, High throughput.

Abbreviations: HTP, High throughput; NanoBiT, Nanoluciferase Binary Technology; ORF, open reading frame; PCA, protein complementation assay; PCR, polymerase chain reaction; PPI, protein-protein interaction; Y2H, yeast-two-hybrid

Abstract

Deciphering protein-protein interactions (PPIs) is crucial for a comprehensive understanding of biological processes, yet current methodologies often provide incomplete interactome maps. Here, we present a sensitive bimolecular NanoBiT-based protein complementation assay platform for robust PPI detection in the fission yeast *Schizosaccharomyces pombe*. Our platform utilizes two NanoLuc moieties, SmBiT and LgBiT, fused to interacting protein partners, generating a quantifiable luminescent signal upon interaction. To maximize the chances of detection and mitigate potential issues arising from tag position-dependent inactivation of bait proteins, our system enables simultaneous expression of two distinct bait constructs within a single cell: one with the LgBiT-tag fused at its N-terminus and another at its C-terminus. For the prey, we constructed a comprehensive ORFeome library of fission yeast proteins, each fused with SmBiT at its C-terminus, leveraging homologous recombination tools. We established efficient high-throughput methods for cloning and selection of single-copy integrants, enabling the rapid construction of the prey library and reliable identification of true yeast transformants. Validating the platform, high-throughput screening using the general transcription elongation factor Tfs1 successfully identified previously undetectable interactors. This versatile platform not only significantly expands the scope of interactome discovery but also offers a powerful tool for future protein-compound interaction studies.

Introduction

As key players in cells, proteins interact with one another to perform and regulate various cellular functions. Thorough detection of these interactions leads to the elucidation of yet understudied biological processes in living organisms. Studying protein-protein interactions (PPIs) is a challenging endeavor not only because proteins can interact with multiple partners, but also because their interactions can be regulated by post-translational modifications (PTMs), cellular localization, and conformational changes[1,2].

The methods for studying PPIs can be classified as biochemical, biophysical, or genetic. Biochemical methods, such as co-immunoprecipitation (based on capturing the interactors with antibodies) and affinity purification coupled with mass spectrometry, are suitable for detecting PPIs *in vitro*[3]. Biophysical techniques, such as surface plasmon resonance, isothermal titration calorimetry, nuclear magnetic resonance, and circular dichroism spectroscopy provide information on the binding affinity, specificity, and kinetics of the interactions. On the other hand, genetic-based methods such as yeast two-hybrid (Y2H)[4], protein complementation assay (PCA)[5,6], Förster (fluorescence) resonance energy transfer (FRET)[7], and bioluminescence resonance energy transfer (BRET)[8], are potent for investigating PPIs *in vivo*. In recent years, the study of PPIs has advanced through the use of expression libraries from various organisms. Among these, the popularity of Y2H[4] for studying PPIs is undeniable due to its scalability and low cost for *in vivo* high-throughput

studies[9,10]. Due to the dynamic nature of the cell[11], however, most interactions fall into the transient and weak category, some of which still remain undetectable by currently available technologies. For instance, current methods, particularly those involving antibodies and tagging, can disrupt native protein interactions under experimental conditions. Such approaches are prone to experimental artifacts and non-specific cross-reactivity within the detection environment, resulting in unreliable false-positive and false-negative outcomes that impede the comprehensive and timely identification of all interacting partners for a given protein.

Protein complementation assays offer several advantages, including a high signal-to-background ratio and stability. One of the most robust classes of luminescence complementation assays is the NanoBiT system. This system is based on a split Nanoluciferase that displays a higher dissociation constant value than most physiological PPIs. It detects physical interactions between two proteins fused with luciferase enzyme moieties, specifically Large BiT (LgBiT: 18 kDa) and Small BiT (SmBiT: 1.3 kDa). Since there is a low affinity between these NanoBiT components, the formation of an active luciferase holoenzyme depends solely on the interaction between the protein pairs attached to them[12].

Generally, yeast cells serve as an ideal model organism due to their conserved basic cellular processes, ease of genetic manipulation, versatile high-throughput platforms, well-characterized genome, ease of culturing and maintenance, available tools and resources, and complementarity with

other attainable systems and model species, as well as their simplification[13]. The fission yeast *S. pombe* holds a wealth of molecular biology tools[14–17], genome-wide deletion collection[18], chemical genomics profiling[19], reverse proteomic data[20], and complete ORFeome library[21]. Additionally, fission yeast often serves as a better model system than budding yeast for studying protein interactions involved in critical biological processes such as gene regulatory events[22]. However, even in the only available comprehensive Y2H study[22] for *S. pombe*, many interactions in certain organelles and with membranous proteins are missing.

In this study, we employed a NanoBiT-based protein complementation assay system in fission yeast to investigate PPIs by incorporating various modifications into the prey and bait expression vectors. A common challenge associated with these assays is the configuration and positioning of tags relative to the protein of interest, primarily due to the limited understanding of structure-activity relationships for most proteins. To address this issue, we expressed two variants of the bait proteins, each with the LgBiT tag fused at a distinct position. A genome-wide screen using the general transcription factor Tfs1 as bait identified over 30 proteins with previously established interactions with Tfs1, demonstrating that the dual-bait strategy is an effective approach for evaluating PPIs.

Materials and Methods

Yeast strains and growth media

The strains used for screening were established by genetic crossing of AM600 (*h⁺ leu1-32 arg3-R25 lys1-K24 ade6-M216*) and AM185 (*h⁹⁰ bfr1::hisG-ura4⁺pmd1::hisG ura4-D18 leu1-32*) strains. Subsequently, the progeny (*h⁺ bfr1::hisG-ura4⁺pmd1::hisG ura4-D18 leu1-32 arg3-R25 lys1-K24 ade6-M216*) was crossed with AM549 (*h⁻ leu1-32 ura4-D18 lys1-K24 ade6-M210*) strain. The screening strain, *h⁺ bfr1::hisG-ura4⁺ pmd1::hisG ura4-D18 leu1-32 arg3-R25 lys1-K24 ade6-M210*, was picked up based on the colony color on the adenine-limited plate, auxotrophy, mating type, and PCR results for *ura4*, *pmd1,* and *bfr1*. Similarly, the counter strain, i.e*., h⁻ mat1<<nat^r bfr1::hisG-ura4⁺ pmd1::hisG ura4-D18 leu1-32 arg3-R25 lys1-K24 ade6-M216* was created by genetic crossing of AM616 (*h⁻ mat1<<nat^r leu1-32 arg3-R25 lys1-K24 ade6-A16*) and AM185 strains. The establishment of *h⁻* strains in which the *mat1* locus was marked by insertion of the natMX marker was described previously[23]. For routine cell culture, YE[24] medium was used. For the selection of transformants and zygotes, selective medium SD, EMM2[24], or EMMG[25] was used. For inducing the expression of transgenes from the *nmt1* promoter, EMM2 or EMMG was used. SPA[24] was used for the induction of sexual differentiation. Adenine, uracil, leucine, lysine, and arginine were added to the medium when needed.

Genetic methods for *S. pombe*

Fission yeast cells were handled as described[24]. For the introduction of the expression plasmids into *S. pombe* cells, each expression plasmid was digested with NotI and subjected to the high-efficiency lithium acetate transformation protocol[26]. A 96-well plate format was used to introduce the expression library into *S. pombe*[27]. The cells were cultured on an SD selective medium supplemented with 50 µg/ml adenine hemisulfate dihydrate (MP biomedicals), L-lysine hydrochloride (Wako), and L-arginine (Wako). The Leu^+ transformants obtained by the introduction of the prey library were exposed to blue/green LED light (FAS-V, NIPPON Genetics). The colonies that clearly showed mCherry fluorescence but had the lowest fluorescence intensity were chosen as transformants having a single copy of the prey construct (see Fig. 3).

Mass mating of the bait- and prey-harboring yeast strains for making diploid cells

To generate diploid strains expressing two baits and each of the prey proteins, the bait-expressing h^+ strain was mated with the prey-expressing *h*⁻ strains. Freshly cultured cells were picked using a 96-pin replicator from solid media and mixed on SPA medium. The cell mixture was re-streaked onto the SD selective medium after two days of incubation at 30 °C[24]. The auxotrophy of bait-expressing strains (leu^- and ade^-) and prey-expressing strains (lys^-, arg^-, and ade^-) was complemented by their counterpart, so that the resulting diploid cells had no auxotrophy.

Construction of a prey vector, pPREY3

A vector for prey expression was constructed based on the pDUAL plasmid, which enables chromosomal integration of a transgene[14]. The EcoRV site (GATATC) in the *leu1* promoter in this plasmid was changed to GATC via inverse PCR so that it would not be recognized by this enzyme. The SacI recognition site (GAGCTC) was deleted by digestion with SacI followed by Klenow fragment treatment and self-ligation. The 3×FLAG tag was introduced between the NheI and BamHI sites by inserting a fragment assembled by annealing of six oligonucleotides (GCTAGCGATATCCATATGGACTACAAGGACCACGACG, CACCAGGAACATCAGGTATACCTATAGCGATCGACGT, GGGATTATAAAGACCACGATATTGATTATAAGGA, ATATTAGTTATAGCACCAGAAATATTAGGGGCAG, TGATGACGATAAACCCGGGTAGCG, and CTAGGCGATGGGCCCAAATAGCAGTAGTAGGA). The recognition sites for EcoRV and NdeI were introduced at this stage. The SmBiT sequence was then inserted just upstream of the 3×FLAG tag sequence via inverse PCR using primers SmBiT-A (TTATCGTTTATTTGAAGAAATTCTCTAGCGGATCCGGCGCGCCA) and SmBiT-B (CTTCAAATAAACGATAACCAGTAACTTTATCGTCATCATCCTTA) followed by gap-repair cloning. The *nmt1* promoter and the ccdB cassette were transferred from pDUAL-FFH1c[14] using SphI and NheI, resulting in

the generation of pDUAL5-ccdB-3F1-SB. The *Cm*^{R} ORF within the ccdB cassette was replaced by the GFP ORF by fusing a GFP-containing fragment to the vector digested with NheI and BglII. The GFP fragment containing a bacterial promoter sequence was generated by two-step PCR. The promoter amplified from pDUAL5-ccdB-3F1-SB using primers Pnmt1-NheI-F (ATAGTCGCTTTGTTAAAGCTAG) and Pcm-GFP-R (CTTCTCCTTTGCTCATAGATCTTTAGCTTCCTTAGCTC), and the GFP ORF amplified from pDUAL-GFH1[14] using primers BglII-GFP-F (AGATCTATGAGCAAAGGAGAAGAACT) and BglII-GFP-R (TAGTAAGCCGGATCCAGATCTTATTTGTATAGTTCATCCATGC), were fused by a second PCR.

The XhoI site in the *leu1* ORF and the EcoRI site flanking the *leu1* ORF were deleted for use in another subcloning. The vector fragment was prepared by digestion with XhoI and EcoRI, and the other fragment was amplified by PCR from the same plasmid using primers CGACCTGAGTTAAAACTCGAATTTGAAGAACACAAGATTGG and TAAAACGACGGCCAGTGAATTGCGGGAGCGCTACCGTGAAT. These fragments were fused by gap-repair cloning. The *ura4*$^{+}$-ars1 fragment was deleted by ApaI digestion followed by self-ligation. The *leu3* promoter was amplified from the wild-type fission yeast genomic DNA by PCR with primers leu3-F1 (GATAACAGGGTAATATACTAGTATGCATAAGAATTGCAAGCC) and leu3-R1 (ACGATTTTCTTTGCACACATGGAGACTGTAGCGATTTTTGGAC).

The mCherry expression unit was transferred from the previously described pBiD3-R25-mCherry vector[28] and inserted upstream of the *nmt1* promoter, in the opposite orientation to the promoter. The promoter was then replaced by the putative constitutive *gpd3* promoter amplified by PCR from the wild-type genome using SphI-Pgpd3-F (AGTCGATCGACCTGCAGGCATGCTCCACGTCTAACCCGCTC) and XhoI-Pgpd3-R (CATCTCGAGTAATTCGATTGCTATTTCTC).

Construction of pXArg3-hLB

The LgBiT fragment, sandwiched between the hexahistidine tag and four consecutive GGGGS linker sequences, was synthesized by artificial gene synthesis (Eurofins Genomics) and inserted between the NheI and BamHI sites of the *lys1*-targeting, pCLys1-derived vector[16]. In analogy to the modification performed in pPREY3, where the ccdB cassette was replaced by GFP, the Cm^R ORF inside the ccdB cassette was substituted with the *mCherry* ORF. The ccdB cassette containing *mCherry* was generated by fusing a PCR product amplified using primer sets Pnmt1-NheI-F (ATAGTCGCTTTGTTAAAGCTAG) and Pcm-mCherry-R (CCTCGCCCTTGCTCACATGCATTTTAGCTTCCTTAGCTC) with the other PCR product generated using CAT-mCherry-F (CATGTGAGCAAGGGCGAGGAGGAT) and BglII-mCherry-R (TAGTAAGCCGGATCCAGATCTTACTTGTACAGCTCGTCCATGC). The NotI and SalI recognition sites within the ccdB cassette were then deleted by

amplifying the mCherry-containing fragment using mCherry-dNotI-F1 (CATATCCAGTCACTATGGCGGCCACATTAGGCACCCCAGGCTTT) and ccdB-dSalI-R1 (CACTATGGTCAACCTGCAGACTGGCTGTGTAT) and ligating the PCR fragment with the same vector used as the template, which was digested with NotI and SalI.

Construction of pXLys1-HA-LB

The other bait-expressing vector, pXLys1-HA-LB, was first constructed based on the pDUAL-type plasmid. This plasmid (pDUAL5-ccdB-4HA1) was formed by replacing the FLAG tag and SmBiT sequence (NdeI-BamHI) of pDUAL5-ccdB-3F1-SB, described above, with four consecutive HA tags. The DNA sequence encoding four copies of the HA epitope was generated by ligating three annealed oligonucleotide pairs. These annealed oligonucleotides were composed of the following sequences: TATGTACCCTTATGATGTACCTGACTACGCCGGC/GCGTAGTCAGGTACATCA TAAGGGTACA, TATCCGTACGACGTCCCAGACTATGCCGGC/GCATAGTCTGGGACGTCGTAC GGATAGCCG, and CCCGGGGAAGAGTACTAGTGG/GATCCACTAGTACTCTTCCCCGGGGCCG. Each pair had cohesive ends that allowed for proper alignment and ligation. One of the oligonucleotide hybrids could be linked in tandem, enabling the generation of more than three copies of the HA epitope. After ligating these fragments with the vector digested with NdeI and BamHI, plasmids

containing four copies of the HA epitope were selected by sequencing from the candidate plasmids. The LgBiT fragment with a termination codon was amplified by PCR using primers NdeI-LgBiT-F (TGGTTGATATCCATATGGTCTTCACACTCGAAGATTT) and NdeI-LgBiT-R (TCATAAGGGTACATATGGCTGTTGATGGTTACTCGG), and was inserted at the NdeI site by a gap-repair technique. Three copies of a GGGGS linker were inserted upstream of the first HA tag by inverse PCR using primers GGGGS2-1-up (AGAGCCTCCACCGCCTGAACTTCCACCGCCTCCAGACATATGGATATCAACC ACT) and GGGGS2-3-down (TCAGGCGGTGGAGGCTCTAGTGGTGGAGGCGGTTCAAATATGTACCCTTAT GATG), followed by gap-repair cloning. A contiguous DNA fragment containing the *nmt1* promoter, ccdB cassette, GGGGS linker, HA tag, and LgBiT was transferred to the pXLys1 vector, a promoter-derivative of the pCLys1 vector having the *lys4* promoter in place of the *lys1* promoter[29]. The ccdB cassette was changed to the mCherry-containing ccdB cassette following the same strategy as pXArg3-hLB.

Quantitative PCR

The copy number of integrated prey-expressing vectors was examined by real-time PCR using a Thermal Cycler Dice Real Time System (TaKaRa Bio). Genomic DNA from the integrants was prepared as described[30] and used as a template. The 3’ part of the *mCherry* ORF was amplified using primers

mCherry-RT-F1 (AAGATGAGGCTGAAGCTGAAG) and mCherry-RT-R1 (GATGGTGTAGTCCTCGTTGTG). Primers act1-RT-F1 (GTTATGTCTGGTGGTACCACT) and act1-RT-R1 (GATCCACCAATCCAGACAGA) were used for amplification of the *act1* gene for data normalization.

Cloning of ORFs into prey and bait expression vectors

For the construction of prey expression plasmids, each ORF from the fission yeast ORF library resource[21] was amplified using universal primers pPREY3-F (CTGACTTATAGTCGCTTTGTTAAAGCTAGCGATATCAAAAAAGCAGGCTCTC ATATG) and pPREY3-R (ATCCCCGTCGTGGTCCTTGTAGTCCATATGGATATCTTTGTACAAGAAAGCT GGGTA) and PrimeSTAR GXL DNA Polymerase (TaKaRa Bio., Japan). The expression plasmids were then constructed by gap-repair cloning in *E. coli* DH5α competent cells by directly introducing each amplified ORF and pPREY3 digested with EcoRV[31]. Similarly, bait plasmids expressing a gene of interest were made by gap-repair cloning using PCR-amplified ORFs and EcoRV-digested pXLys1-HA-LB or SmaI-digested pXArg3-hLB. The universal primers for inserting the gene of interest into pXLys1-HA-LB were pXLys1-F (CTGACTTATAGTCGCTTTGTTAAAGCTAGCGATATCAAAAAAGCAGGCTCTC ATATG) and pXLys1-HA-LB-R (GCCTGAACTTCCACCGCCTCCAGACATATGGATATCTTTGTACAAGAAAGCT

GGGTA). The forward universal primer for amplification of a gene of interest for insertion into pXArg3-hLB (N-tagged vector) was: GGAGGCGGTTCAGGAGGCGGAGGCTCAGATCCCGGGAAAAAAGCAGGCTCT CATATG. The reverse primer with the stop codon sequence was designed specifically for each gene of interest.

Luciferase assay

The freshly grown fission yeast cells were picked from YE agar plates (pre-culture) and inoculated into 1 ml of EMMG medium[24,25] in a 96-deep-well plate (Nunc™ 96-well Polypropylene DeepWell™ Storage Plates; Thermo Scientific), which was then incubated at 30 °C for 20 hours. Cells were then harvested and suspended in 12 µl of fresh EMMG medium. Subsequently, a volume of 12 µl of cell suspension was transferred to assay plates (384-well cell culture microplates, F-bottom, white, Greiner, Bio-One), and mixed with 11.85 µl of Y-PER™ Plus Dialyzable Yeast Protein Extraction Reagent (Thermo Scientific) detergent and 0.15 µl of Furimazine (or 2-furanylmethyl-deoxycoelenterazine, Nano-Glo Luciferase Assay Substrate Promega Corp.) solution. Just before measurement of the luciferase activity by an EnSpire Multimode plate reader (Perkin Elmer), the mCherry fluorescence signal (i.e., $\lambda_{excitation}$ = 587 nm & $\lambda_{emission}$ = 610 nm) was measured using a SpectraMax M2/M2^{e} microplate reader (Molecular devices, LLC).

335 **Statistical analysis**

336 In this study, the results of three technical replicates were calculated as
337 mean values with error bars (corresponding to ± standard deviation/SD).
338 The significance of each experiment was statistically validated using a two-
339 tailed unpaired Student's *t*-test in Microsoft Excel (Microsoft 365), with *p*-
340 values ($p < 0.05$) obtained.

Results

The strategies of the NanoBiT-based PCA system in this study

To meet the need for more sensitive PPI detection systems in *S. pombe*, where well-established molecular biology tools are already available, we developed a NanoBiT-based protein complementation assay (PCA) system. This system utilizes the LgBiT moiety of deep-sea shrimp luciferase and its complementary peptide, SmBiT. However, a major challenge in *S. pombe* is the lack of detailed structure-activity relationship data for most proteins, which complicates the determination of optimal fusion points for the LgBiT/SmBiT fragments. To address this challenge, we expressed the protein of interest as two distinct baits, each fused differently with the LgBiT tag (Fig. 1A). This strategy aimed to reduce the risk of missing potential positive interactions, based on the hypothesis that positive signals could be detected from at least one of the bait constructs (Fig. 1B). This would hold true even if one bait construct led to steric hindrance or suboptimal positioning of the interacting fragments. To expand the utility of this system not only for given bait proteins, but also for genome-wide screening, we designed three integration vectors targeting different genomic loci and developed host strains compatible with these expression plasmids, enabling the simultaneous expression of two baits and one prey, as detailed below (Fig. 1C).

Construction of vectors for bait expression; pXArg3-hLB and pXLys1-HA-LB

In this assay, the arrangement and the order of LgBiT in a bait protein posed a significant challenge as described above. Therefore, we partially addressed this issue by expressing a bait protein as two differently tagged plasmids. Among several possible ways to express one protein as two different constructs, e.g. bait proteins fused with LgBiT having different length linkers, we chose to express two bait proteins with LgBiT fused to either N- or C-terminus.

To establish a binary system featuring dual orientations of tagging, we employed two vectors containing the LgBiT fragment of the NanoLuc luciferase. Accordingly, we integrated the LgBiT fragment into two distinct vectors: pXArg3, a modified variant of the pCArg3 vector targeting the *arg3* locus, and pXLys1, a modified version of the pCLys1 vector, targeting the *lys1* locus[29]. The introduction of NotI-digested pCLys1-derived vector into the *lys1* locus, bearing the *lys1-K24* mutation, yielded a functional *lys1* gene, resulting in lysine prototrophic transformants. We employed a similar approach for pCArg3-derived vectors, which restored the *arg3-R25* mutation upon chromosomal integration. To reduce steric hindrance between the LgBiT fragment and the protein of interest, tandem glycine and serine linkers were introduced between the LgBiT fragment and each ORF in the bait vectors. Additionally, small epitope tags, specifically the HA epitope or the hexahistidine tag, were incorporated into the vectors to

facilitate the detection of the bait expression. Both baits were expressed under the control of the thiamine-repressible *nmt1* promoter, enabling inducible, controllable expression by thiamine limitation. Consequently, two distinct bait-expressing vectors were constructed: pXArg3-hLB for 5'-tagging, and pXLys1-HA-LB for 3'-tagging (Fig. 1B).

Construction of a prey expression vector, pPREY3

To facilitate the rapid and straightforward cloning of the fission yeast ORFeome and the subsequent expression of prey constructs through chromosomal integration, we developed a prey expression vector based on the chromosomal integration vector pDUAL, targeting the *leu1* locus. Although pDUAL vectors have the *ura4* and ars1 sequences that enable episomal maintenance in host cells, we deleted these sequences from the vector backbone to ensure prey proteins are expressed only from the chromosome in this system.

We included multiple design elements in the prey-expression vector to obtain yeast transformants expressing desired prey constructs. Notably, we occasionally encounter a problem where yeast transformants fail to express a transgene introduced by single-crossover recombination using integration vectors such as pDUAL, which may be attributed to further recombination between a pair of repeated sequences generated upstream and downstream of the inserted fragment[32]. On the other hand, another general problem when introducing transgenes using integration plasmids is multiplication of

inserted fragments[29]. To obtain reproducible and quantitative outcomes, it is necessary to select transformants with an equivalent copy number of the integrated gene. The copy number or expression level of the introduced gene can be verified using standard techniques such as quantitative PCR and western blotting. However, when using numerous samples as in the genome-wide screening, a practical expedient suited to the high-throughput systems is needed.

To solve these concerns simultaneously, we included an *mCherry* expression unit driven under the regulation of the constitutive *gpd3* (glyceraldehyde 3-phosphate dehydrogenase) promoter in the prey-expression vector (Fig. 2). Expression of *mCherry* was easily monitored by directly observing the fluorescence of transformant colonies on the agar plate under LED light exposure, thereby eliminating transformants with no insertion. In addition, transformants exhibiting strong mCherry fluorescence, expected to have multiple copies of the insertion, can also be eliminated. As confirmed by real-time qPCR, the expression levels of *mCherry*, monitored by fluorescence, correlated with the copy number of *mCherry* in the genome (Fig. 3). Transformants that clearly exhibited mCherry fluorescence but showed the weakest fluorescence were picked as those having only one copy of the prey ORF (Fig. 3). Implementing high-throughput screening using optical density (OD) measurements proved operationally cumbersome due to the tendency of cells to sink during

manipulation. As a solution to this issue, the mCherry signal served as the basis for normalizing data in luciferase assays.

For fast and effective cloning, we have also included a technical feature in this vector to increase the probability of obtaining *E. coli* transformants harboring desired plasmids (Fig. 2). The Gateway-compatible pDUAL vectors contain a stuffer named the ccdB cassette[33], which is composed of the toxic *ccdB* gene and the chloramphenicol resistance gene (Cm^R). We replaced the Cm^R ORF, which is non-essential for cloning, with that of GFP. By this approach, intact vectors (without inserts) were eliminated by two selection criteria: the *ccdB* ORF and GFP tracking of bacterial transformants. Although the CcdB protein is toxic to standard laboratory *E. coli* strains, we often encounter a problem where *E. coli* transformants harboring the ccdB plasmid can grow, probably due to mutations or rearrangements occurring in the plasmid. Even when *E. coli* hosts harboring the unreacted vector are viable, such transformants can be identified by GFP fluorescence and eliminated. Conversely, when the GFP-ccdB cassette is properly replaced with an ORF, the fluorescence is lost in the transformants, making it easier to determine if the desired transformants have been obtained.

By inserting the SmBiT fragment into the vector having the above properties, we successfully constructed a vector referred to as pPREY3 (Fig. 2). The prey proteins were also expressed under the control of the thiamine-repressible *nmt1* promoter. The existing ORFeome library[21] was used to

prepare the prey expression library by 3’-tagging with SmBiT. Although we cloned the ORFeome library into pPREY3 mainly via gap-repair cloning, the Gateway-cloning system provides an alternative in case gap-repair cloning is unsuccessful. As a result of selecting transformants, a set of yeast haploid strains transformed with more than 97% of the prey library constructs derived from the available ORFeome library were successfully obtained. For the selection of counter strains expressing bait proteins, we confirmed the expression of the baits by performing western blotting.

Establishment of *S. pombe* strains for NanoBiT-based PCA

To identify proteins that interact with a protein of interest, it is necessary to generate a collection of strains expressing two baits and each of approximately 5,000 preys. While the introduction of three expression plasmids into the genome of a host strain is feasible, this approach has limited applicability because the strain set cannot then be used to screen interactions with other protein targets. To address this issue, we employed intragenic complementation of the two *ade6* alleles, *ade6-M210* and *ade6-M216*, in which one serves as a host for prey library constructs and the other as a host expressing bait proteins. In the realm of fission yeast research, it is widely recognized that diploid cells carrying both *ade6-M210* and *ade6-M216* alleles do not exhibit adenine auxotrophy. This characteristic allows for the straightforward selection and maintenance of Ade^+ zygotes resulting from the mating of adenine-

auxotrophic *ade6-M210* and *ade6-M216* haploids[25,34]. In addition, while the prey-expression vector pPREY3 restores leucine auxotrophy, two baits that are introduced by pXLys1 and pXArg3 complement lysine and arginine auxotrophy, respectively. Thus, auxotrophy for all four nutrients was restored after zygote formation in combination with the intragenic complementation of *ade6-M210* and *ade6-M216* alleles.

To further expand the range of applications, we deleted *bfr1* and *pmd1* both encoding efflux pumps[35], as deletion of both *bfr1* (brefeldin resistance)[36] and *pmd1* (leptomycin transmembrane transporter)[37] confers sufficient drug sensitivity[35]. By incorporating this gene disruption, the assay system can accommodate cases in which protein-protein interactions require the intervention of specific compounds such as the FK506-FKBP12-calcineurin complex.

Validation of established NanoBiT-based PCA in fission yeast using known interactions

To determine whether the PCA system consisting of the vectors and the host strains described above works well, we conducted luciferase assays using representative proteins with known interactors. When *rad24* was introduced using bait vectors for either N- or C-terminal tagging with LgBiT, the N-terminally tagged Rad24 (LB-Rad24) exhibited higher luciferase activity compared to the C-terminally tagged variant (Rad24-LB) (Fig. 4A). Notably, the combination of LB-Rad24 with Plc1 (Plc1-SB) or Fft3

(Fft3-SB) produced strong luciferase signals, whereas Rad24-LB paired with the same prey proteins showed activity at background levels. For example, the signal from self-interaction between LB-Rad24 and Rad24-SB was higher than that from the interaction between LB-Rad24 and Prz1-SB. However, this relationship was reversed when Rad24-LB was used instead of LB-Rad24. These results strongly suggest that the ability to detect protein-protein interactions depends highly on the orientation of the interacting proteins and the position of the tag, similar to what is observed in Y2H. Thus, if one construct fails to detect an interaction, the other may compensate for this limitation. The use of two bait proteins with different tag positions is therefore an effective strategy for enhancing the detection of interactions within the system.

To further evaluate the effectiveness of expressing two bait proteins with different tag positions, we examined their simultaneous expression — specifically, both N- and C-terminal fusions, which are independently active. As shown in Fig. 4B, the co-expression of LB-Mms1 and Mms1-LB with Ubc13-SB resulted in higher luciferase activity compared to the expression of either bait alone. This additive effect indicates that simultaneous expression of two baits with different orientations of LgBiT fusion improves the detectability of protein-protein interactions, further validating the versatility and reliability of the system.

Building on the effectiveness of this dual-bait expression strategy, we evaluated whether our PCA system could detect interactions involving

proteins that are typically challenging to analyze using conventional Y2H assays, such as membrane-associated proteins. As a proof of concept, we selected several membrane-associated amino acid transporters and assessed their interactions with known interacting partners, including Pub1, an E3 ubiquitin-protein ligase complex subunit (Fig. 4C). Our system successfully detected these interactions, demonstrating its ability to overcome the limitations of traditional Y2H systems.

A genome-wide interaction study

To explore and delve deeper into the potential of our NanoBiT-based system, we sought to identify novel interactors of a protein that was tested in another genome-wide system. To do so, we developed a high throughput platform for PPI studies. We selected Tfs1, a general transcription elongation factor, as a bait protein to explore its interactors. This protein has many already-identified interactors[22], thereby providing a good basis for comparison between the hit proteins obtained in this system and the known interacting partners. We expressed Tfs1 as two separate baits, each tagged with the LB tag fused to either the N- or C-terminus of the protein. The strain expressing two Tfs1 baits was mated with a set of strains expressing the 4,662 ORFeome preys, and the zygotes were examined for luciferase activity.

This screen identified 31 proteins that exhibited significantly strong luciferase activity, including known interactors such as Tvp15 (COPI-coated

vesicle associated protein), Ecm31 (3-methyl-2-oxobutanoatehydroxymethyltransferase), Vps20 (ESCRT III complex subunit), and Yop1 (ER membrane protein), thereby affirming the system's reliability (Fig. 5A, Supplementary Table 1). Notably, only 9 interactors overlapped with those previously reported by Vo et al. (2016), suggesting that each methodology captures a distinct subset of interactions (Fig. 5B). This observation is consistent with findings from Ito et al. (2001), who emphasized the complementary nature of different interaction-detection methods.

It is conceivable that both methodologies include numerous false positives or transient, non-specific interactions influenced by specific experimental conditions or functional contexts. Nevertheless, the screen identified 22 proteins whose interactions with Tfs1 were previously unreported, as shown in Fig. 5B.

NanoBiT-based PCA, the screening system used in this study, can detect interactions that are difficult for Y2H systems to detect, as the bait-prey interaction is not confined to specific cellular compartments. Noteworthy examples of identified interactors located beyond the nucleus include the mitochondrial protein Mtq1 (mitochondrial N(5)-glutamine methyltransferase), the NADHX epimerase Mug182, and the ER/cell wall protein Spbp23a10.11c (circularly permuted 1,3-beta-glucanase). The latter two are also involved in stress responses.

Discussion

In this study, we developed a NanoBiT-based platform for detecting PPIs, building upon the existing pDUAL vector system[14,16], and leveraging the genetic tools and strains of *S. pombe*. We modified the pDUAL vectors to include NanoBiT components, selectable markers, and elements supporting efficient screening across multiple workflow stages. Notably, the pPREY3 vector enabled high-efficiency cloning of the fission yeast ORFeome, while the pXLys1-HA-LB and pXArg3-hLB vectors allowed bait protein expression in two alternative tag configurations. These configurations address structural or functional uncertainties by offering flexibility in tag positioning. In parallel, we generated compatible fission yeast strains that support dual-bait co-expression, thereby expanding the range of detectable interactions.

These features highlight the versatility and sensitivity of our PCA system, particularly in detecting transient or weak PPIs often missed by conventional methods such as the traditional Y2H system. The combination of dual-bait expression and flexible tagging improves detection of biologically relevant interactions, making our system a valuable tool for dissecting complex interaction networks. Following successful detection of known interactions, including those involving membrane-associated proteins, we applied the system in a genome-wide screen to identify novel interactors of the transcription elongation factor Tfs1. Although Tfs1 is primarily nuclear, increasing evidence suggests that transcription factors can shuttle between the nucleus and cytoplasm, especially under stress conditions. TFIIS family

members, including the Tfs1 homolog TFIIS.h (human ortholog), have been implicated in stress responses[38], genome maintenance[39], and transcriptional recovery[40], in part via phase separation[41,42]. These findings raise the possibility that Tfs1 participates in broader regulatory roles beyond its nuclear function, which may be governed by post-translational modifications or subcellular sequestration. The ability to detect Tfs1-associated interactions by our system supports its utility for capturing such dynamic, context-dependent PPIs.

While our high-throughput screen identified promising candidate interactors of Tfs1, co-immunoprecipitation assays for selected pairs were inconclusive, likely due to the transient or weak nature of these interactions. Notably, false-positive and false-negative results are a common concern not only in NanoBiT assays but also in other split-based systems, such as split-GFP or split-ubiquitin, as well as in Y2H. This limitation highlights a key advantage of our PCA-based approach, which is optimized to detect conditionally assembled, low-affinity, or modification-dependent interactions often missed by traditional methods like co-IP or Y2H. Nevertheless, the possibility remains that some of the identified candidates may represent false-positive interactions inherent to split-based assays. In addition, it is important to note that the NanoBiT assay cannot provide information about the subcellular localization of these interactions. Potential ectopic interactions—whether due to assay artifacts or unexpected biological phenomena—cannot be evaluated with this system. Therefore, further

validation using orthogonal methods, such as co-immunoprecipitation, pull-down assays, or microscopy-based colocalization, will be essential to confirm the physiological relevance of these interactions.

Importantly, several of the identified candidates overlapped with interactors reported in previous global Y2H studies, lending orthogonal support to our findings. This reinforces the biological relevance of our data and suggests that our system efficiently captures interaction partners that may be inaccessible to methods reliant on stable complex formation. Given the limitations of biochemical approaches for studying dynamic PPIs, our platform offers a complementary—and in some cases superior—strategy for mapping interaction networks, especially for proteins like Tfs1 that may function in multiple cellular compartments.

Looking ahead, the modularity of our system opens avenues for further innovation. One direction is the development of a three-hybrid system to detect compound-protein interactions. This would involve a modified HaloTag[43] protein fused to LgBiT, which recruits a small molecule that bridges to an SmBiT-tagged target, thereby reconstituting luciferase activity. Our prey-expressing strains are compatible with this approach through the use of counter-strains expressing HaloTag fusions, allowing versatile compound positioning.

Additionally, the absence of drug efflux pumps in our strains makes them ideal for small-molecule screening. This supports both the identification of

PPI modulators and target proteins, positioning our system as a powerful tool for drug discovery. With continued development, we anticipate that our platform will advance the understanding of complex protein interactions and accelerate both basic and translational research.

Acknowledgement

This work was supported by the Japan Society for the Promotion of Science (JSPS) KAKENHI Grant Numbers 22K05361 and 23H05473 and by the Ministry of Education, Culture, Sports, Science and Technology (MEXT) KAKENHI Grant Number 23H04882 for Transformative Research Areas (A). Grammar and linguistic refinement of this manuscript were kindly assisted by Gemini 1.5 Pro (Google Cloud AI Studio).

Author Contributions

This work was conceptualized by A.M. and M.Y. All experiments were done by A.M., A.H., and F.A. A.M. and F.A. prepared the original draft. S.N., M.A. and M.Y. edited the manuscript. All authors reviewed the manuscript.

Competing Interests

The authors declare no financial conflicts of interest.

Funding

This work was supported by the Japan Society for the Promotion of Science (Grant Number: 22K05361 and 23H05473), and the Ministry of Education, Culture, Sports, Science and Technology (Grant Number: 23H04882). The authors declare that no other funding was received for this study.

Data Availability Statement

The authors confirm that all data required to support the conclusions of this article are included within the text, figures, and tables. Protein–protein interaction screening data generated using the NanoBiT system in this study have been submitted to the IMEx (http://www.imexconsortium.org) consortium through IntAct [X][44] and assigned the identifier IM-30540. Strains and plasmids are available upon request or from the Yeast Genetic Resource Center (YGRC/NBRP) of Japan.

References

1. De las rivas, J. & Fontanillo, C. Protein-protein interaction networks: Unraveling the wiring of molecular machines within the cell. *Brief. Funct. Genomics* **11**, 489–496 (2012).
2. Tsai, C. J., Ma, B. & Nussinov, R. Protein-protein interaction networks: how can a hub protein bind so many different partners? *Trends Biochem. Sci.* **34**, 594–600 (2009).
3. Titeca, K., Lemmens, I., Tavernier, J. & Eyckerman, S. Discovering cellular protein-protein interactions: Technological strategies and opportunities. *Mass Spectrom. Rev.* **38**, 79–111 (2019).
4. Fields, S. & Song, O. K. A novel genetic system to detect protein-protein interactions. *Nature* **340**, 245–246 (1989).
5. Tebo, A. G. & Gautier, A. A split fluorescent reporter with rapid and reversible complementation. *Nat. Commun.* **10**, 2822 (2019).
6. Pelletier, J. N., Campbell-Valois, F. X. & Michnick, S. W. Oligomerization domain-directed reassembly of active dihydrofolate reductase from rationally designed fragments. *Proc. Natl. Acad. Sci. U. S. A.* **95**, 12141–12146 (1998).
7. Algar, W. R., Hildebrandt, N., Vogel, S. S. & Medintz, I. L. FRET as a biomolecular research tool — understanding its potential while avoiding pitfalls. *Nat. Methods* **16**, 815–829 (2019).
8. Xu, Y., Piston, D. W. & Johnson, C. H. A bioluminescence resonance energy transfer (BRET) system: Application to interacting circadian

clock proteins. *Proc. Natl. Acad. Sci. U. S. A.* **96**, 151–156 (1999).

9. Ito, T. *et al.* A comprehensive two-hybrid analysis to explore the yeast protein interactome. *Proc. Natl. Acad. Sci. U. S. A.* **98**, 4569–4574 (2001).
10. Yu, H. *et al.* High-quality binary protein interaction map of the yeast interactome network. *Sci. AAAs* **322**, 104–110 (2008).
11. Hofmann, J. L., Maheshwari, A. J., Sunol, A. M., Endy, D. & Zia, R. N. Ultra-weak protein-protein interactions can modulate proteome-wide searching and binding. *bioRxiv* (2022). doi:10.1101/2022.09.30.510365
12. Dixon, A. S. *et al.* NanoLuc Complementation Reporter Optimized for Accurate Measurement of Protein Interactions in Cells. *ACS Chem. Biol.* **11**, 400–408 (2016).
13. Vyas, A., Freitas, A. V., Ralston, Z. A. & Tang, Z. Fission Yeast *Schizosaccharomyces pombe*: A Unicellular “Micromammal” Model Organism. *Curr. Protoc.* **1**, e150 (2021).
14. Matsuyama, A. *et al.* pDUAL, a multipurpose, multicopy vector capable of chromosomal integration in fission yeast. *Yeast* **21**, 1289–1305 (2004).
15. Matsuyama, A., Shirai, A. & Yoshida, M. A novel series of vectors for chromosomal integration in fission yeast. *Biochem. Biophys. Res. Commun.* **374**, 315–319 (2008).
16. Matsuyama, A., Hashimoto, A., Nishimura, S. & Yoshida, M. A set of vectors and strains for chromosomal integration in fission yeast. *Sci. Rep.* **13**, 315–9 (2023).

17. Shirai, A. *et al.* Global analysis of gel mobility of proteins and its use in target identification. *J. Biol. Chem.* **283**, 10745–10752 (2008).

18. Kim, D. U. *et al.* Analysis of a genome-wide set of gene deletions in the fission yeast *Schizosaccharomyces pombe*. *Nat. Biotechnol.* **28**, 617–623 (2010).

19. Nishimura, S. *et al.* Marine antifungal theonellamides target 3β-2-hydroxysterol to activate *Rho1* signaling. *Nat. Chem. Biol.* **6**, 519–526 (2010).

20. Bauer, F. *et al.* Translational Control of Cell Division by Elongator. *Cell Rep.* **1**, 424–433 (2012).

21. Matsuyama, A. *et al.* ORFeome cloning and global analysis of protein localization in the fission yeast *Schizosaccharomyces pombe*. *Nat. Biotechnol.* **24**, 841–847 (2006).

22. Vo, T. V. *et al.* A proteome-wide fission yeast interactome reveals network evolution principles from yeasts to human. *Cell* **164**, 310–323 (2016).

23. Ohsawa, S. *et al.* Nitrogen signaling factor triggers a respiration-like gene expression program in fission yeast. *EMBO J.* **43**, 4604–4624 (2024).

24. Forsburg, S. L. & Rhind, N. Basic methods for fission yeast. *Yeast* **23**, 173–183 (2006).

25. Petersen, J. & Russell, P. Growth and the environment of *Schizosaccharomyces pombe*. *Cold Spring Harb. Protoc.* **2016**, (2016).

26. Matsuyama, A., Yabana, N., Watanabe, Y. & Yamamoto, M. *Schizosaccharomyces pombe* Ste7p is required for both promotion and withholding of the entry to meiosis. *Genetics* **155**, 539 (2000).

27. Shirai, A., Matsuyama, A., Yashiroda, Y., Arai, R. & Yoshida, M. Rapid and reliable preparation of total cell lysates from fission yeast. *Protoc. Exch.* (2006).

28. Chiu, P. C. *et al.* Ferrichrome, a fungal-type siderophore, confers high ammonium tolerance to fission yeast. *Sci. Rep.* **12**, (2022).

29. Matsuyama A, Hashimoto A, Arioka M, Y. M. Improvement of Targeting Efficiency by Promoter Replacement of Markers in Integration Vectors. *Genes Cells* **30**, e70013 (2025).

30. Hoffman, C. S. Preparation of Yeast DNA. *Curr. Protoc. Mol. Biol.* **39**, 13–11 (1997).

31. Jacobus, A. P. & Gross, J. Optimal cloning of PCR fragments by homologous recombination in *Escherichia coli*. *PLoS One* **10**, e0119221 (2015).

32. Keeney, J. B. & Boeke, J. D. Efficient targeted integration at leu1-32 and ura4-294 in *Schizosaccharomyces pombe*. *Genetics* **136**, 849–856 (1994).

33. Bernard, P. & Couturier, M. Cell killing by the F plasmid CcdB protein involves poisoning of DNA-topoisomerase II complexes. *J. Mol. Biol.* **226**, 735–45 (1992).

34. Reaume, S. E. & Tatum, E. L. Spontaneous and nitrogen mustard-

766 induced nutritional deficiencies in. *Arch. Biochem.* **22**, 331–338 (1949).
767 35. Arita, Y. *et al.* Microarray-based target identification using drug
768 hypersensitive fission yeast expressing ORFeome. *Mol. Biosyst.* **7**,
769 1463–1472 (2011).
770 36. Nagao, K. *et al.* bfr1^{+} a novel gene of *Schizosaccharomyces pombe*
771 which confers brefeldin A resistance, is structurally related to the ATP-
772 binding cassette superfamily. *J. Bacteriol.* **177**, 1536–43 (1995).
773 37. Nishi, K. *et al.* A leptomycin B resistance gene of *Schizosaccharomyces*
774 *pombe* encodes a protein similar to the mammalian P-glycoproteins. *Mol.*
775 *Microbiol.* **6**, 761–9 (1992).
776 38. Papadopoulos, D. *et al.* MYCN recruits the nuclear exosome complex to
777 RNA polymerase II to prevent transcription-replication conflicts. *Mol.*
778 *Cell* **82**, 159-176.e12 (2022).
779 39. Zatreanu, D. *et al.* Elongation Factor TFIIS Prevents Transcription
780 Stress and R-Loop Accumulation to Maintain Genome Stability. *Mol. Cell*
781 **76**, 57-69.e9 (2019).
782 40. Siametis, A. *et al.* Transcription stress at telomeres leads to cytosolic
783 DNA release and paracrine senescence. *Nat. Commun.* **15**, 4061 (2024).
784 41. Cho, W. K. *et al.* Mediator and RNA polymerase II clusters associate in
785 transcription-dependent condensates. *Sci. AAAs* **361**, 412–415 (2018).
786 42. Göös, H. *et al.* Human transcription factor protein interaction networks.
787 *Nat. Commun.* **13**, 766 (2022).
788 43. Ohana, R. F. *et al.* HaloTag7: A genetically engineered tag that enhances

bacterial expression of soluble proteins and improves protein purification. *Protein Expr. Purif.* **68**, 110–20 (2009).

44. del Toro, N. *et al.* The IntAct database: efficient access to fine-grained molecular interaction data. *Nucleic Acids Res.* **50**, D648–D653 (2022).

Figure Legends

Figure 1. Schematic of NanoBiT-based PCA system and the designed vectors in fission yeast

A) The scheme of the NanoBiT-based PCA system, comprising a bait protein fused to the LgBiT fragment of NanoBiT system having either 3’ or 5’ tagging and prey proteins fused to the SmBiT moiety. Upon interactions of ORF1 (bait) and ORF2 (prey), the full-length luciferase enzyme is formed and produces a luminescence signal.

B) The structure of bait plasmids. The interactors of a protein of interest are introduced by separate vectors as both 3’- and 5’-tagged using the pDUAL-based[14] vectors with LgBiT fragment into separate loci of yeast chromosome. ORF, open reading frame; LB, LargeBiT, h, hexahistidine tag; GS, GGGGS linker; HA, HA epitope.

C) The scheme of an *S. pombe* cell with indicated target loci. Three marker loci targeted by integration plasmids are indicated on each chromosome of fission yeast. cen, centromere.

Figure 2. Features and structure of pPREY3 vectors.

Plasmid map indicating various components of the pPREY3 vector, including GFP expression gene inside the ccdB cassette and the ampicillin resistance gene. There is also an mCherry expression unit independent of

the components required for expression of a transgene, used to quantify the level of expression of each transgene.

Figure 3. Correlation between genomic *mCherry* copy number and fluorescence intensity.

(Top) Scatter plot showing the relationship between the relative genomic copy number of the *mCherry* gene and its fluorescence intensity. The *mCherry* copy number was normalized to that of the endogenous *act1* gene using quantitative real-time PCR. Fluorescence intensity was normalized to cell density (OD_{600}). Each data point represents an independent transformant generated by pPREY3 integration. The plot reveals a positive correlation between normalized *mCherry* copy number (*mCherry*/*act1*) and normalized fluorescence intensity (mCherry fluorescence/OD_{600}), indicating that observed fluorescence reflects integrated *mCherry* copy number. A trendline is indicated by a dashed line.

(Bottom) mCherry fluorescence of pPREY3 integrants used for qPCR, observed under blue/green LED light. Cells at positions C10-12 correspond to the host strains lacking the *mCherry* expression unit.

Figure 4. Feasibility pilot experiments for testing the NanoBiT-based PCA system.

A) Rad24 (14-3-3 protein) was chosen as a hub protein and some of its known interactors, i.e., Rad24 (14-3-3 protein), Plc1 (phosphoinositide

phospholipase C), Prz1 (calcineurin responsive DNA-binding transcription factor), and Fft3 (histone chaperone/ATP-dependent chromatin remodeler) were examined. The bait was cloned into pXLys1-HA-LB and pXArg3-hLB vectors. Error bars represent the standard deviation ($n = 3$, Error bars are SD of mean, *** indicates $p < 0.001$, **** indicates $p < 0.0001$, two-sample t-test assuming unequal variances). Strains having an empty vector (-) or expressing GFP were used as negative controls. Negative controls are indicated with grey color.

B) The effect of signal intensity when using a bait in two different orientations of tagging. Here, Ubc13 (ubiquitin conjugating enzyme E2) is used as a prey protein and its interaction with the bait protein, Mms2 (ubiquitin conjugating enzyme E2), as C-tagged, N-tagged, and C, N-tagged was tested. Error bars represent the standard deviation ($n = 3$, * indicates $p < 0.05$, *** indicates $p < 0.001$, two-sample t-test assuming unequal variances). Strains expressing GFP served as negative controls. For baits, a "(-)" indicates the absence of a plasmid, while for preys, it signifies an empty vector. Negative controls are highlighted in grey.

C) Luciferase assay using a bait in two different orientations of tagging. Several transmembrane proteins whose rare interactors were available in PomBase were selected, including Spbc1652.02, Isp5, Aat1, Cat1 as amino acid transporters, and Pub1 as a ubiquitin-protein ligase E3. Cut11 (spindle pole body docking protein), Any1 (arrestin-related

substrate adaptor), Ubi4 (protein modifier, ubiquitin), and Ptr2 (plasma membrane PTR family peptide transmembrane transporter). Error bars represent the standard deviation (n = 3, ns: not significant, ** indicates $p < 0.01$, *** indicates $p < 0.001$, two-sample t-test assuming unequal variances). Strains having an empty vector (-) were used as negative control and are indicated with grey color.

Figure 5. A high-throughput screening using Tfs1 as a bait protein in NanoBiT-based PCA.

A) High-throughput screening for Tfs1-interacting proteins. The graph plots the $\log_{10}$-transformed luciferase activity for each tested ORF, which are ranked from lowest to highest activity. Colored triangles indicate positive hits with a p-value < 0.05 (n = 9).

B) The comparison of the screening performed in this study with the previous Y2H study[22]. The screenings share the following hit proteins: Ecm31 (3-methyl-2-oxobutanoatehydroxymethyltransferase), Omt2 (4-alpha-hydroxytetrahydrobiopterin dehydratase), Tvp15 (COPI-coated vesicle associated protein), Dal81 (DNA-binding transcription factor), Vps20 (ESCRT III complex subunit), Yop1 (ER membrane protein), Ndk1 (nucleoside diphosphate kinase), Spac1f7.10 (hydantoin racemase family), and Spcc576.02 (hydantoin racemase family).

885

886

887 **Supplementary Table 1. List of proteins identified as interacting**

888 **with Tfs1.**

889 Genes encoding proteins identified as interacting with Tfs1 in this study

890 (NanoBiT-PCA) and in the Y2H system. A “+” symbol indicates detection of

891 interaction in each experimental system.

892

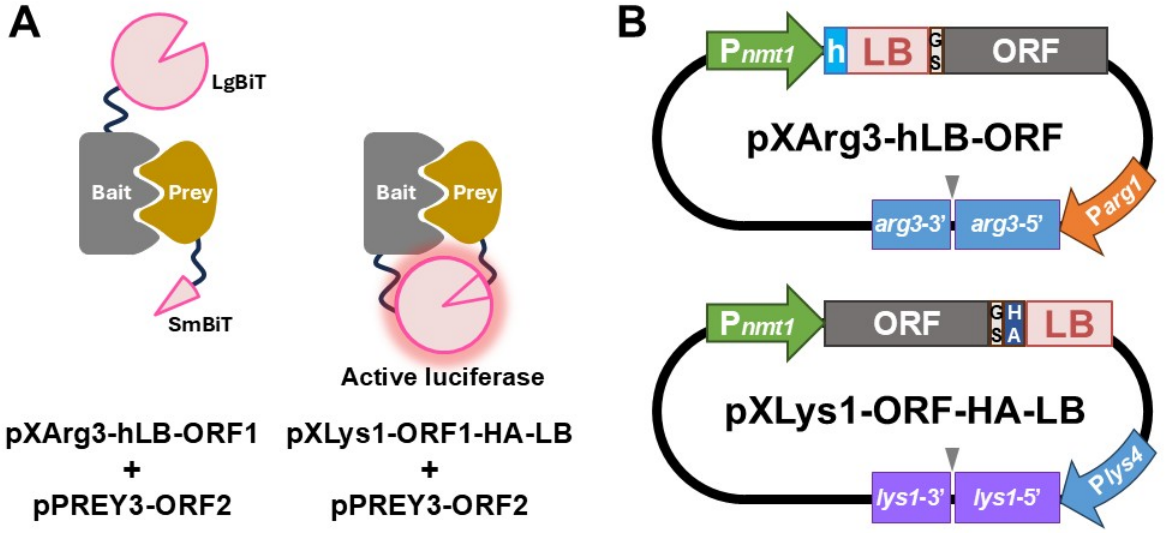

Figure 1A, B

893

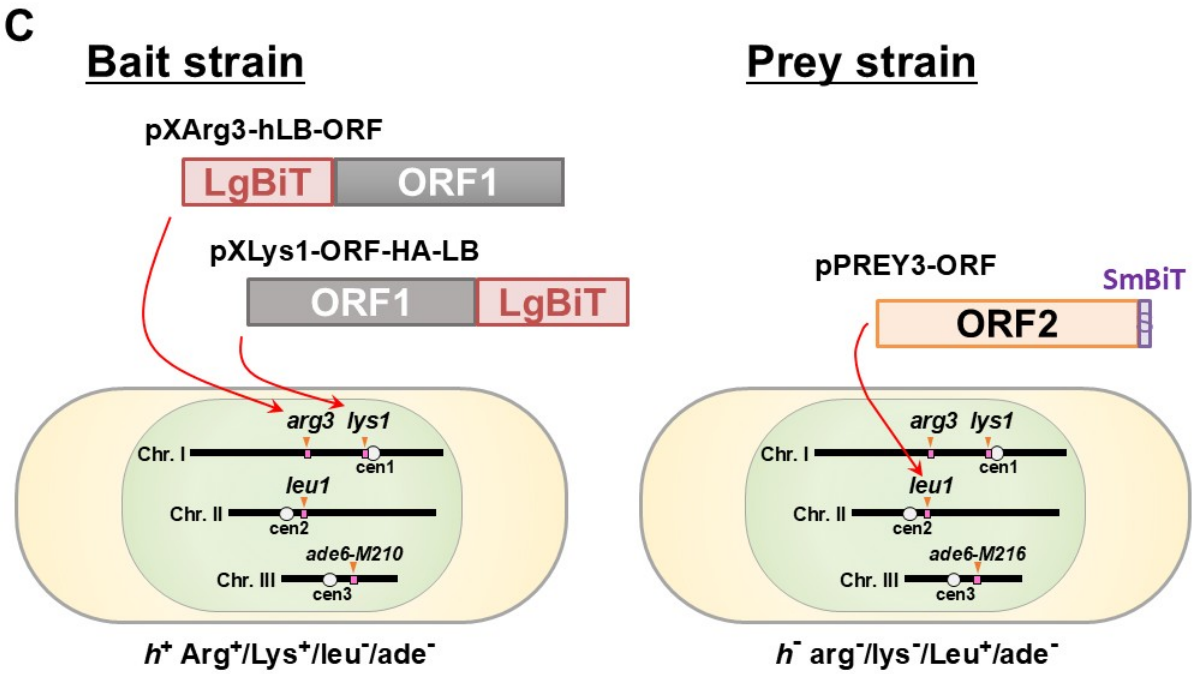

Figure 1C

894

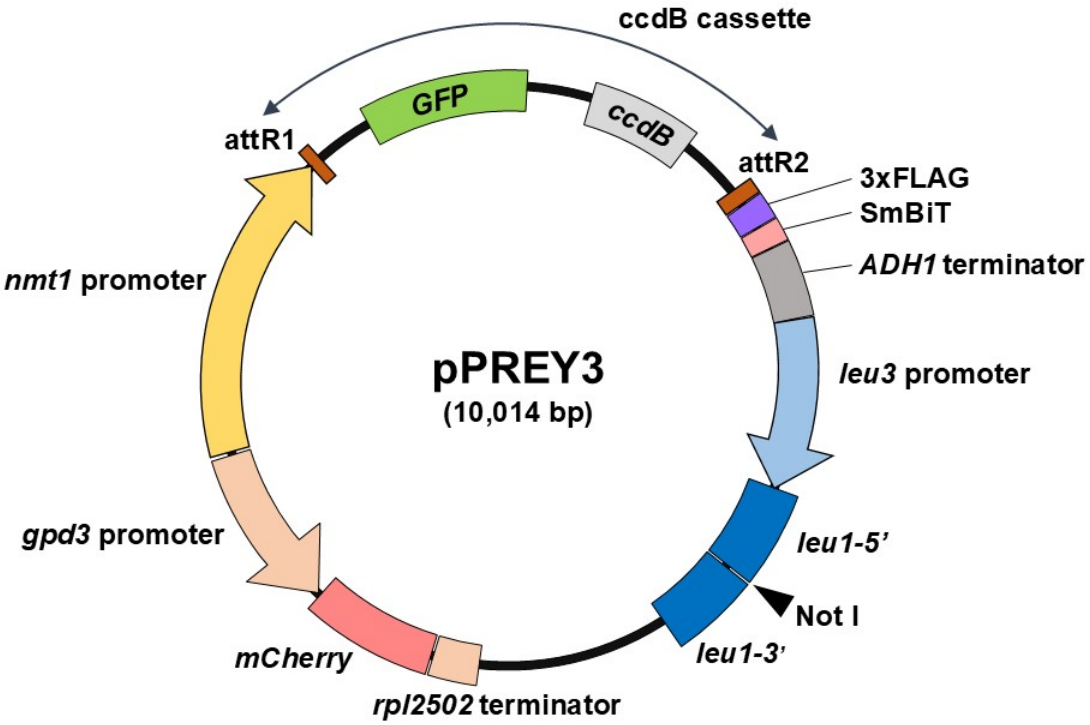

Figure 2

895

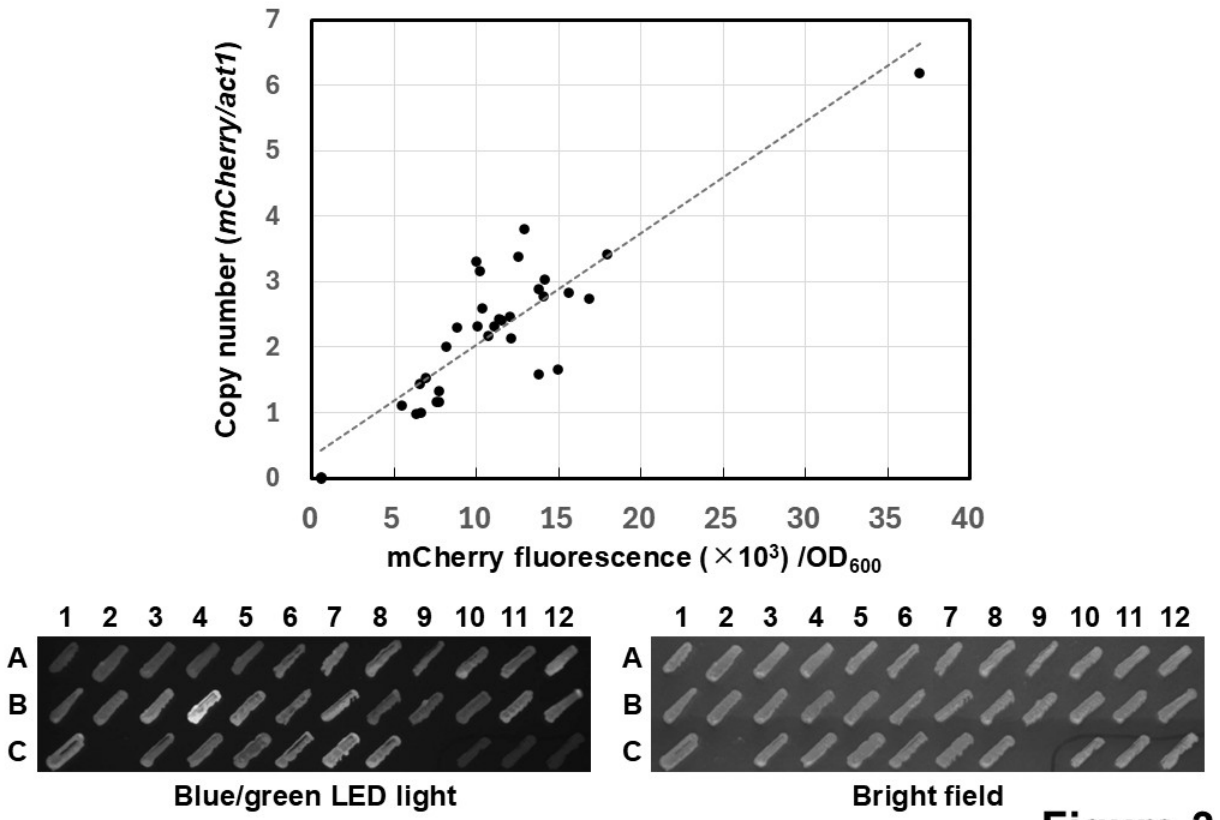

Figure 3

896

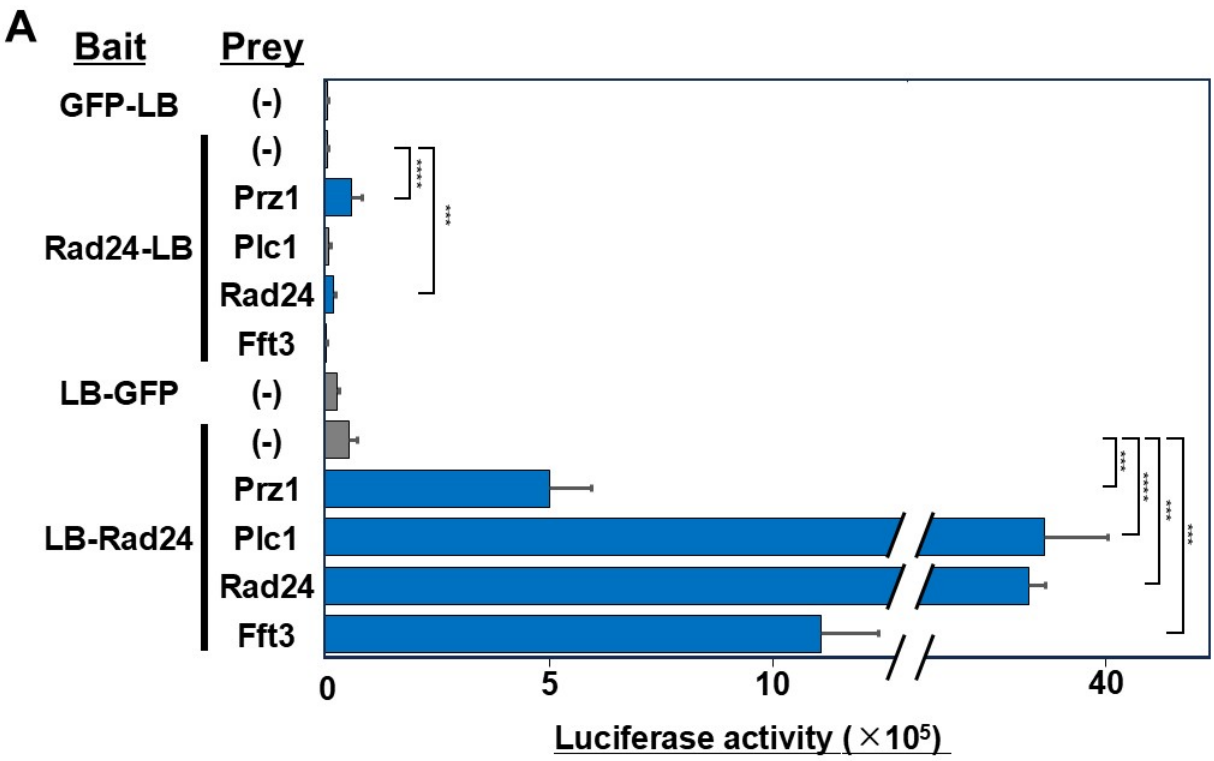

Figure 4A

897

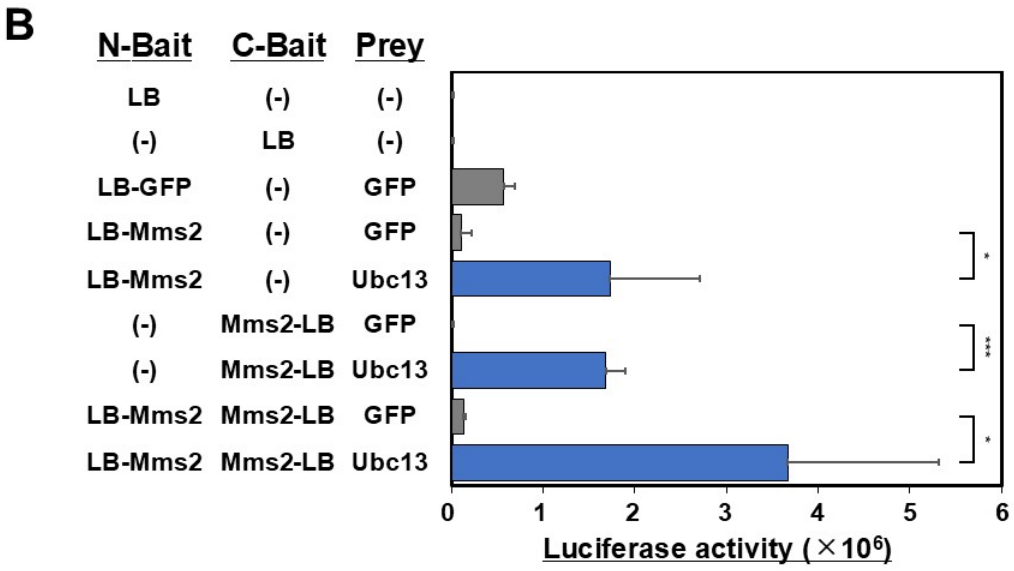

Figure 4B

898

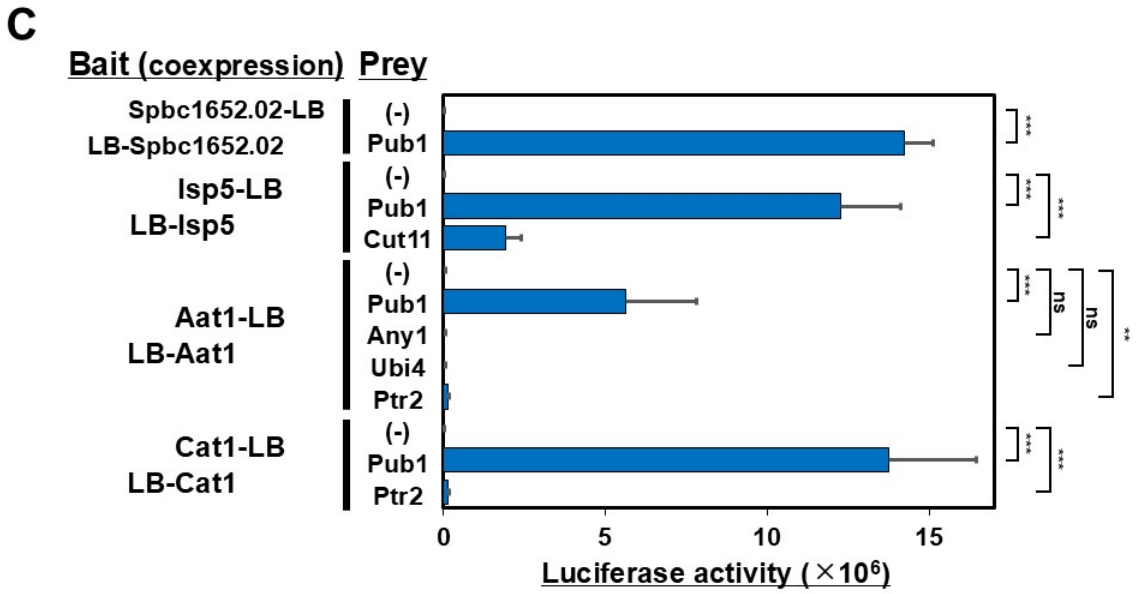

Figure 4C

899

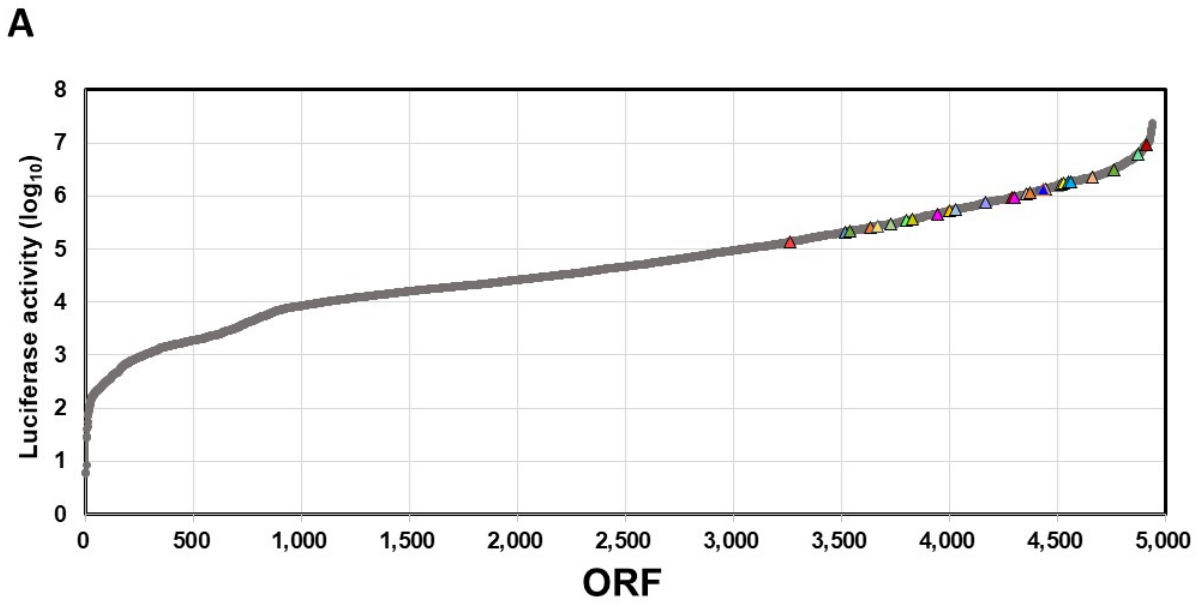

Figure 5A

900

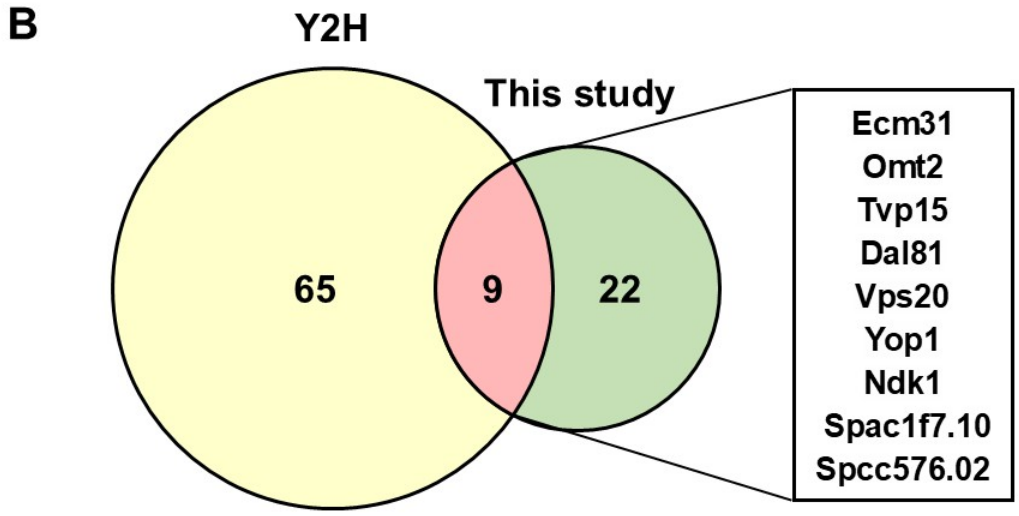

Figure 5B

901